© 2015. Published by The Company of Biologists Ltd | Development (2015) 142, 1937-1947 doi:10.1242/dev.104802

REVIEW

The origin of the mammalian kidney: implications for recreating the kidney *in vitro*

Minoru Takasato[1,2] and Melissa H. Little[1,2,*]

ABSTRACT

The mammalian kidney, the metanephros, is a mesodermal organ classically regarded as arising from the intermediate mesoderm (IM). Indeed, both the ureteric bud (UB), which gives rise to the ureter and the collecting ducts, and the metanephric mesenchyme (MM), which forms the rest of the kidney, derive from the IM. Based on an understanding of the signalling molecules crucial for IM patterning and kidney morphogenesis, several studies have now generated UB or MM, or both, *in vitro* via the directed differentiation of human pluripotent stem cells. Although these results support the IM origin of the UB and the MM, they challenge the simplistic view of a common progenitor for these two populations, prompting a reanalysis of early patterning events within the IM. Here, we review our understanding of the origin of the UB and the MM in mouse, and discuss how this impacts on kidney regeneration strategies and furthers our understanding of human development.

KEY WORDS: Kidney development, Directed differentiation, Mesoderm, Nephrogenic mesenchyme, Pluripotent stem cell, Ureteric bud, Stem cells

Introduction

At the end of 2013, the global number of individuals being treated for end-stage renal disease (ESRD) was estimated at ~3.2 million, with a 6.3% annual growth rate; significantly higher than the world population growth rate (1.1%) (http://www.vision-fmc.com/files/ESRD_Patients_in_2013.pdf). Despite this, organ transplantation or dialysis remain the only therapies available to treat individuals with ESRD. A source of stem cells able to recreate the functional units of the kidney, the nephrons, does not exist in the adult organ, as the embryonic nephron progenitor population of the human kidney is exhausted by birth (Hinchliffe et al., 1991). Although the equivalent population in mouse persists for the first few days of life (Hartman et al., 2007; Rumballe et al., 2011), it also exhausts, which results in an inability to generate new nephrons in response to postnatal injury. Whereas the nephron progenitor population can be isolated from the mouse embryonic kidney, raising the prospect of nephrogenesis *in vitro*, access to nephron progenitors from human embryonic kidney is impractical and ethically challenging. An alternative is the recreation of nephron progenitors from human pluripotent stem cells (hPSCs).

Since the observation that the introduction of key reprogramming transcription factors enabled the generation of human induced-pluripotent stem cells (iPSCs) (Takahashi et al., 2007), protocols for their directed differentiation have been established for various organs. Directed differentiation of hPSCs towards kidney has now been reported by a number of groups (Mae et al., 2013; Xia et al., 2013; Taguchi et al., 2014; Takasato, 2014a; Lam et al., 2014). Although these all drew on knowledge of the molecular regulation of kidney development, the end results and their interpretation varied. This suggests a need for a careful reanalysis of our current understanding of kidney development. In this Review, we will revisit what we understand about the origin of this mesodermal organ in the mouse, discuss how well the directed differentiation of human pluripotent stem cells (hPSCs) recapitulates this process, and describe what implications this has on our capacity to harness hPSCs for regenerative medicine and on our understanding of normal human development.

Kidney morphogenesis in mammals

The mammalian kidney, the metanephros, comprises complex epithelial tubules, the nephrons, that filter the blood to remove waste and reabsorb water and nutrients to maintain homeostasis. The human kidney contains up to 2 million nephrons per organ (Bertram et al., 2011), whereas in the mouse this number is around 15,000 (Merlet-Bénichou et al., 1999). Each nephron connects with the collecting duct network through which the urinary filtrate passes to exit the kidney and move to the bladder (Fig. 1).

The formation of the nephrons and the collecting ducts occurs as the result of reciprocal interactions between two key embryonic compartments derived from the intermediate mesoderm (IM), the metanephric mesenchyme (MM) and the ureteric bud (UB) (Fig. 1). The UB arises as a side branch of the nephric duct (ND), also called the mesonephric duct or the Wolffian duct (Little et al., 2007), which arises prior to pronephros induction and extends caudally to connect eventually with the forming bladder. The UB grows towards the MM in response to the glial cell-derived neurotrophic factor produced within the mesenchyme (Fig. 1). As the UB reaches the MM, it begins a program of dichotomous branching to form the collecting ducts of the final organ (Short et al., 2014). During that process, a subset of the MM – the cells closest to the tips of the branching UB – becomes the cap mesenchyme (CM), a self-renewing population of cells able to both support continued UB branching and give rise to nephrons (Fig. 1). The surrounding MM gives rise to the stromal and vascular elements of the organ, including the capillaries of the glomeruli (Little and McMahon, 2013).

During the first stage of nephron formation, driven by the production of WNT9B from the UB tip (Carroll et al., 2005), the CM undergoes a mesenchyme-to-epithelial transition (MET) and aggregates into a renal vesicle (Fig. 1). Each renal vesicle then elongates, becomes segmented and gives rise to all cell types within the final nephron (Fig. 1). Hence, waves of nephron induction and continued UB branching occur simultaneously to generate the final organ.

Three pairs of kidneys form from the IM

Metanephric morphogenesis has been extensively studied. However, although the paired metanephroi represent the permanent kidneys

[1]Institute for Molecular Bioscience, The University of Queensland, St. Lucia, Queensland 4072, Australia. [2]Murdoch Children's Research Institute, Royal Children's Hospital, Parkville, Victoria 3052, Australia.

*Author for correspondence (melissa.little@mcri.edu.au)

Development (2015) 142, 1937-1947 doi:10.1242/dev.104802

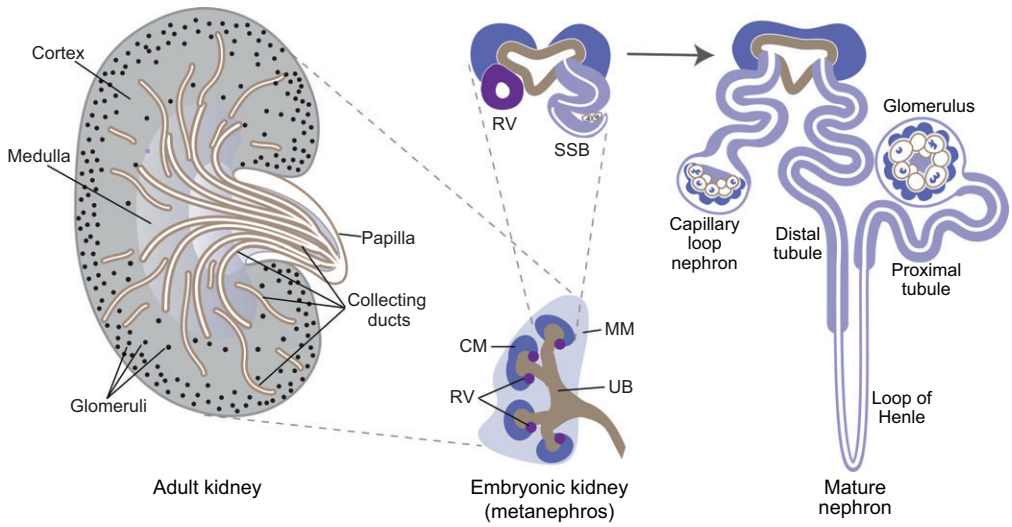

Fig. 1. The developing kidney in the mouse. The adult mouse kidney, patterned into an external cortex, containing glomeruli, the medulla and a single papilla, through which the collecting ducts drain. The metanephros arises from the ureteric bud (UB, brown), an epithelial sidebranch from the nephric duct and the metanephric mesenchyme (MM, light blue). As the UB branches within the MM, those MM cells closest to the UB form the cap mesenchyme (CM, dark blue) from which the nephrons arise via a mesenchyme-to-epithelial transition. These are first recognizable as renal vesicles (RVs, purple), as shown in the diagram. Within each ureteric tip/cap mesenchyme niche, RV undergo elongation and segmentation into S-shaped bodies (SSBs). These elongate further to establish a capillary loop before maturing to include a loop of Henle (mature nephron).

during postnatal mammalian life, they are actually the last of three pairs of excretory organs that form from the IM. These form along the antero-posterior (A-P) axis of the embryo in a distinct temporal sequence (pronephros, mesonephros and metanephros from rostral to caudal) and the first two organs degenerate during embryonic life (Fig. 2A-C) (Saxen, 1987). This order also represents an evolutionary sequence. Indeed, cyclostomes (primitive aquatic vertebrates) form only the pronephros, which they use throughout life. Fishes and amphibians form the pronephros and the mesonephros, the latter functioning as the adult kidney.

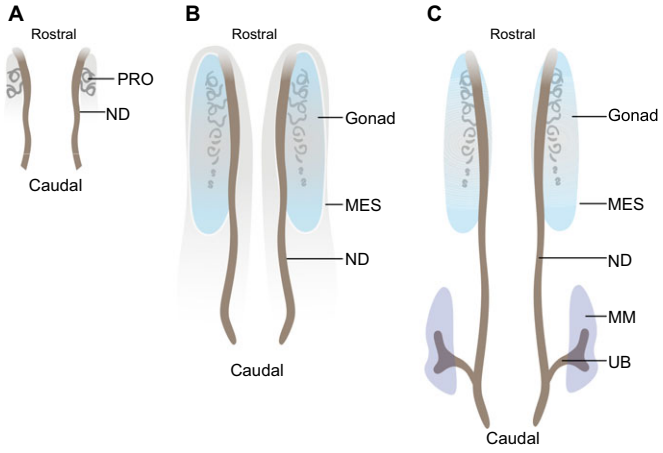

Fig. 2. Formation of the three pairs of excretory organs during mammalian development. (A) The pronephros (PRO) develops at the rostral end of the IM in humans at embryonic day 22 (E8.0 in mice) along the nephric duct (ND). (B) The mesonephros (MES) forms posterior to the pronephros from day 24 in humans (E9.0 in mice). This organ develops nephrons that drain directly into the nephric duct and is associated closely with the developing gonad (light blue). The mesonephros and pronephros degenerate with remaining mesonephric ducts contributing to the male reproductive tract. (C) The metanephros forms from day 35 (week 5) in humans (E10.5-E11 in mice) and arises at the level of the hindlimbs. The UB branches off the ND and grows into the MM.

All three excretory organs drain into the ND and also have cellular components that arise from the nephrogenic mesenchyme (NM) flanking the ND. In humans, the pronephros develops at the rostral end of the IM by embryonic day 22 (E8.0 in mice), with only rudimentary tubules opening into the ND (Vetter and Gibley, 1966) (Fig. 2A). The human mesonephros begins to form caudally to the pronephros from day 24 of gestation (E9.0 in mice), the gonad arising from an adjacent region of the IM (Fig. 2B). Similar to the metanephros, the mammalian mesonephros has nephrons containing vascularized glomeruli connected to proximal and distal tubules that empty directly into the ND (Woolf, 2009; Vetter and Gibley, 1966). Indeed, the temporal and spatial gene expression seen in the nephrons of the mesonephros is very similar to that seen in the metanephros (Georgas et al., 2011). Finally, the metanephros forms at the caudal end of the IM from embryonic day 35 (E10.5 in mice) (Fig. 2C).

Thus, A-P patterning of the IM is crucial to specify each of these distinct pairs of organs, and this process is particularly important if we hope to specifically recreate the metanephros. However, there has been little investigation of the cues that distinguish the processes of morphogenesis between the three excretory organs in mammals.

Rostral cell migration from the pre-somitic mesoderm generates trunk mesoderm

Understanding how the distinct pairs of urinary organs arise requires a comprehension of how the IM itself arises from part of the pre-somitic mesoderm (PSM). Taken literally, the term PSM should apply only to the progenitors of the somites; however, this term has been widely used to describe the embryonic tailbud or the posterior nascent mesoderm domain that gives rise to all trunk mesoderm, including the IM. In this Review we will also use the term ‘PSM’ to indicate embryonic tailbud or posterior nascent mesoderm. All three excretory organs originate from this population.

The trunk mesoderm, including the IM, is derived from the primitive streak via the PSM. Using DiI labelling and time-lapse imaging within the tailbud of the developing chicken embryo, it was demonstrated that PSM cells migrate in a rostral direction towards the head of the embryo (James and Schultheiss, 2003; Sweetman et al.,

Development (2015) 142, 1937-1947 doi:10.1242/dev.104802

2008) (Fig. 3A). During embryonic trunk elongation, PSM cells divide, continually pushing out the daughter cells towards the rostral region. After migration, these daughter cells differentiate into paraxial mesoderm (PM; which forms somites), IM and lateral plate mesoderm (LPM; which forms muscular and skeletal elements) (Fig. 3A,B). This experiment on chick embryos also showed that the PM is derived from the anterior region of the PSM domain, whereas the LPM is generated from the posterior PSM, thus confirming previous studies (Kinder et al., 1999, 2001; Parameswaran and Tam, 1995). This caudal-to-rostral cell migration can be described differently if viewed from the level of the rostral trunk. From the rostral trunk point of view, both rostral and caudal trunk mesoderm is moving caudally as the axis of the embryo elongates, with relative movement of the caudal cells faster than that of rostral cells due to differences in cell density between rostral and caudal regions (Bénazéraf et al., 2010). Conversely, this can be viewed as cell migration from caudal to rostral from the PSM point of view (Bénazéraf et al., 2010).

The migration of PSM cells is driven by a chemotactic response to fibroblast growth factor (FGF) signalling through fibroblast growth factor receptor 1 (FGFR1), present on PSM cells. FGF4 is expressed by the forming somites and acts as a chemoattractant, attracting PSM daughter cells rostrally (Fig. 3B). Conversely, FGF8 from the PSM, signalling through MAPK (mitogen-activated protein kinase), works as a chemorepellent, stimulating the migration of daughter cells away from the PSM (Fig. 3B) (Shamim and Mason, 1999; Yang et al., 2002; Delfini et al., 2005; Bénazéraf et al., 2010; Boulet and Capecchi, 2012).

However, FGF is not the only chemotactic signal regulating PSM cell migration. Platelet-derived growth factor α (PDGFA), which is secreted by the rostral trunk, also induces PSM cell migration via platelet-derived growth factor receptor α (PDGFRA) (Fig. 3B). In response to PDGFA, PSM cells express N-cadherin (*Cdh2*), an essential molecule for this cell migration (Tallquist et al., 2000; Yang et al., 2008). Indeed, mouse embryos lacking *Cdh2* are embryonic lethal (by E10) and show somite disorganization and cell-adhesion defects in the primitive heart (Horikawa et al., 1999; Radice et al., 1997), consistent with a malformation of the early mesoderm.

WNT signalling is also a potential regulator of PSM cell migration. Both *Wnt3a* and *Wnt5a* are expressed in the PSM but in slightly different patterns (Fig. 3B) (Yoshikawa et al., 1997; Yamaguchi et al., 1999; Sweetman et al., 2008). *In situ* hybridization data shows that *Wnt3a* is mainly expressed in the anterior PSM that gives rise to the paraxial mesoderm (PM), with weaker expression in the posterior PSM that generates the IM and/or LPM. By contrast, *Wnt5a* expression is detected throughout the PSM. Sweetman et al. (2008) performed the aforementioned DiI tracing experiments and time-lapse imaging to investigate PSM cell migration in the presence of various WNT-soaked beads. They reported that this difference in *Wnt3a* and *Wnt5a* expression pattern actually coordinates PSM cell migration; the WNT5A-mediated PCP pathway is required for dynamic cell migration from the posterior PSM, whereas WNT3A-mediated canonical WNT signalling antagonizes WNT5A signalling-driven cell migration but regulates the convergent extension of the PM. Indeed, *Wnt3a* mutant mice display a caudally truncated embryo primarily due to the failure of PM organization (Takada et al., 1994; Yoshikawa et al., 1997; Dunty et al., 2008), whereas *Wnt5a* mutant mice show a reduction in the size of the caudal body (Yamaguchi et al., 1999).

The temporal sequence of PSM migration dictates IM regionalization

Having described the signals that regulate the migration capacity and direction of cells located in the different regions of the PSM, it is important to consider the temporal aspect of this process. Indeed, PSM daughter cells that migrate rostrally in the early stages of IM formation give rise to rostral IM, whereas those migrating out later give rise to caudal IM.

The mesoderm marker brachyury (*T*) is expressed in the primitive streak and persists in the PSM. In the E8.5 mouse embryo, *T* is expressed in the node, the PSM and at low levels in daughter cells migrating from the PSM (Galceran et al., 2001). In mouse, lineage tracing of T^+ cells was investigated using *T-CreERT2×Rosa26-LacZ*, Tomato or YFP mice in which T^+ cells are permanently marked after tamoxifen injection (Anderson et al., 2013; Taguchi et al., 2014; Yun et al., 2014). As *T* is expressed in the whole primitive streak at E7.5, trunk cells from tail to neck, including the heart, limbs and trunk mesoderm, were all marked after a tamoxifen injection at E7.5. By contrast, when the injection was carried out at E8.5 or E9.5, only the caudal half or the tail end of the embryo was marked, respectively. In other words, daughter cells migrating rostrally from the PSM between E7.5 and E8.5 give rise to the rostral half of the embryo, including the heart and forelimbs, whereas static cells or cells that initiate their migration at E8.5 give rise to the caudal half of the embryo, including the hindlimbs and the mesonephric and

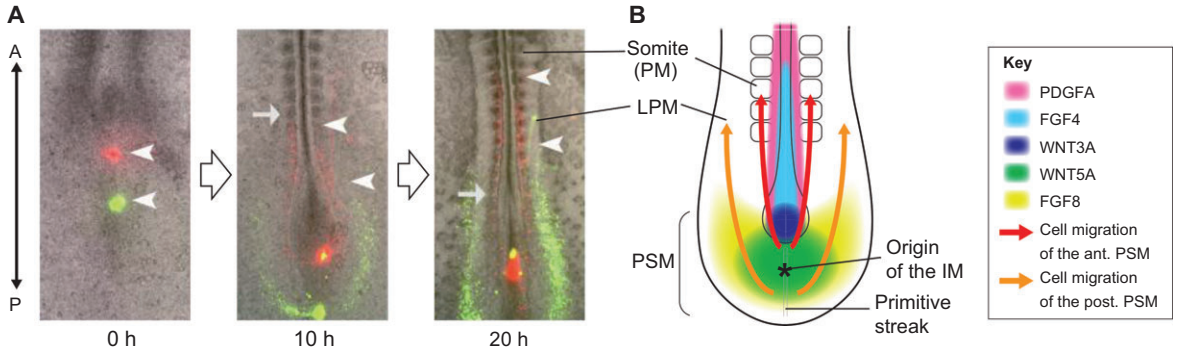

Fig. 3. Regulation of cell migration from the presomitic mesoderm (PSM). (A) Still images extracted from a 20 h time-lapse video of the chick embryo streak at stage HH7-9 where the anterior part was labelled with DiI (red) and the posterior region was marked with DiO (green), show the cell movement of paraxial and lateral plate mesoderm progenitors. White arrows indicate the most recently formed somite; arrowheads indicate the most anterior DiI- and DiO-labelled cells that have left the primitive streak. A, anterior; P, posterior. Reproduced, with permission, from Sweetman et al. (2008). (B) Candidate factors that regulate cell migration of the pre-somitic mesoderm (PSM) in mouse at E8.0-E8.5. Each coloured field represents a domain secreting the factor indicated. Red and orange arrows represent the path of cell migration from the anterior and posterior PSM, respectively. Asterisk represents a region in the PSM that gives rise to the intermediate mesoderm (IM) after cell migration. LPM, lateral plate mesoderm; PM, paraxial mesoderm.

Development (2015) 142, 1937-1947 doi:10.1242/dev.104802

metanephric regions; finally, PSM cells at E9.5 contribute only the very tail end of the embryo. Interestingly, tamoxifen injections at E8.5 revealed that the ND, even within the metanephric region, was not marked, indicating that it arises earlier than this time. Conversely, the MM was marked, suggesting derivation from the post E8.5 PSM (Taguchi et al., 2014). Together, these observations suggest that while the ND arises from the IM, it is early rostral IM established prior to the IM that gives rise to the MM.

The expression pattern of the homeobox-containing (Hox) gene family, which is highly conserved among the deuterostomes, also support this temporal sequence (Fig. 4). During patterning of the body plan, Hox genes show a strict temporal and spatial patterning. The best example of this is seen during mesoderm segmentation and somitogenesis. Hox genes from the 3′ end of the gene cluster (lower numbered paralogues) initially express in early posterior primitive streak, followed by expression of more 5′ Hox genes (higher numbered paralogues) as development progresses towards later stages of primitive streak (Forlani et al., 2003; Kmita and Duboule, 2003; Deschamps and van Nes, 2005; Soshnikova and Duboule, 2009). This differential gene expression across time is converted to a spatial pattering of Hox gene expression along the A-P axis of the embryo trunk (Fig. 4). Such a distinct spatial Hox gene expression pattern is also seen in the formation of the excretory system. In the developing chick embryo, *Hoxb4* expression marks the anterior boundary of the IM (Preger-Ben Noon et al., 2009), whereas *Hoxa6* is expressed just posterior to the IM region, from where the ND arises (Attia et al., 2012). Subsequently, *Hoxb7* and *Hoxd8* are expressed in the ND, whereas *Hoxc10*, *Hoxa11*, *Hoxc11*, *Hoxd11* and *Hoxd12* are expressed in the MM (Kress et al., 1990; Patterson and Potter, 2004). Interestingly, the MM shows differential expression of *Hox11* paralogues with respect to the more rostral mesonephros (Wellik et al., 2002; Challen et al., 2004), thus also supporting an earlier origin for the ND versus the MM.

A-P regulation of the fate of early versus late migrating mesoderm

Although the regulation of A-P patterning related to paraxial mesoderm somitogenesis has been well investigated (Dubrulle et al., 2001; Naiche et al., 2011), what morphogens are involved in the determination of the rostral versus caudal fate of the IM? Here, we focus on two signalling pathways, retinoic acid (RA) and FGF signalling, which generate opposing gradients along the rostrocaudal axis during development.

RA signalling is a well-known regulator of mesoderm segmentation during embryogenesis (Duester, 2008). RA is synthesized by enzymes such as ALDH1A2 (aldehyde dehydrogenase family 1, subfamily A2) in the anterior trunk of the embryo from the primitive streak stage. Hence, a gradient of RA activity extends from the rostral end of the embryo (Fig. 5A). *Aldh1a2* mutant mice display a failure of proper segmentation of the anterior trunk mesoderm (Niederreither et al., 1999) but maintain a relatively normal posterior body plan, except for the absence of the nephric duct. This indicates that RA is required for rostral IM specification. In fact, in a gain-of-function experiment, RA can indirectly upregulate the rostral IM marker *Lhx1* through *Hoxb4* expression in the rostral IM region (Preger-Ben Noon et al., 2009). Conversely, suppression of RA signalling is required for normal development of the mesoderm in the posterior region of the embryo (Abu-Abed et al., 2001; Sakai et al., 2001). RA signalling reporter (RARE-LacZ) mice show no RA activity in the PSM (Rossant et al., 1991). This is because *Cyp26a1*, an enzyme that metabolizes RA, is expressed in that region, acting as a sink to shield PSM cells from the influence of RA (Fig. 5A). When *Cyp26a1* was genetically mutated, RA signalling was ectopically activated in the PSM, resulting in a caudally truncated embryo (Abu-Abed et al., 2001; Sakai et al., 2001). In these mice, a metanephric kidney still forms; however, the two kidneys are fused and only one medially positioned nephric duct is present, suggesting aberrant cell migration from the PSM. Therefore, it is reasonable to postulate that cells are instructed to differentiate into IM in response to RA signalling soon after emerging from the

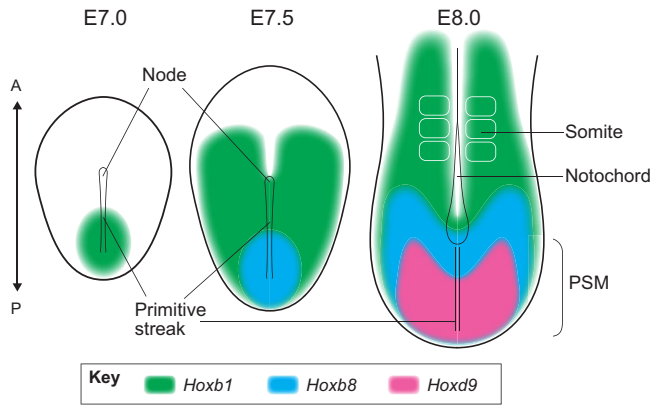

Fig. 4. Temporal sequence of Hox gene expression and spatial patterning of the trunk along the A-P axis. The expression patterns of *Hoxb1* (green), *Hoxb8* (blue) and *Hoxd9* (pink) as examples of three differently numbered Hox paralogues during early mouse embryogenesis at E7.0, E7.5 and E8.0. *Hoxb1* is expressed in the posterior end of primitive streak from E7.0, and thus contributes to the rostral body patterning at the later stage. By contrast, *Hoxb8*, which is expressed from E7.5, is expressed caudally to the *Hoxb1*$^{+}$ domain, as shown in E8.0. The expression of *Hoxd9*, the 5′-most Hox gene of these three, follows half a day after *Hoxb8*, resulting in a three-color pattern along the A-P axis (E8.0). PSM, pre-somitic mesoderm.

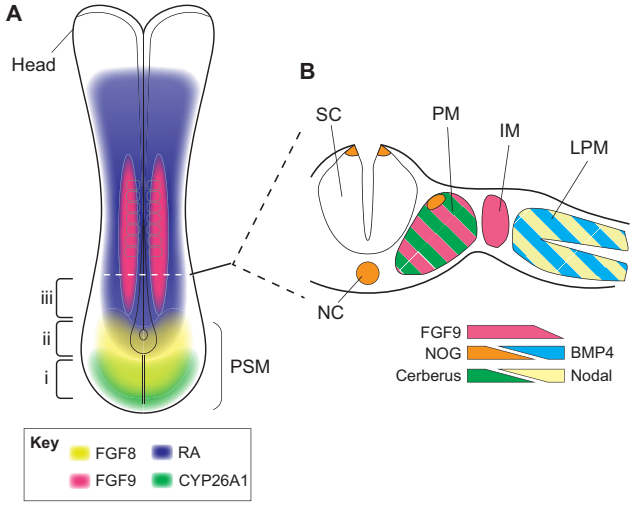

Fig. 5. Morphogens specifying mesoderm along the mediolateral and anteroposterior axis. (A) Diagram illustrating morphogen gradients of A-P patterning regulators in a stage E8.5 mouse embryo, including FGF8 (yellow), FGF9 (pink), RA (blue) and CYP26A1 (green). Three domains of influence are indicated from caudal to rostral: (i) RA-nonresponding/FGF8-responding domain; (ii) RA-responding/FGF8-responding domain and (iii) RA-responding/FGF8-nonresponding domain. (B) Cross-section of the embryo axis at the position indicated in A (dotted line) illustrating the expression of regulators of M-L patterning: FGF9 (pink), noggin (NOG, orange), BMP4 (blue), cerberus (green) or nodal (cream). Actual morphogen gradients are illustrated below. The thickness of bars represents the level of activity of each morphogen. IM, intermediate mesoderm; LPM, lateral plate mesoderm; NC, notochord; PM, paraxial mesoderm; PSM, pre-somitic mesoderm; SC, spinal cord.

Development (2015) 142, 1937-1947 doi:10.1242/dev.104802

Cyp26a1^{+} PSM region. Hence, the cells that migrate from the PSM at late stages and give rise to the caudal IM spend a substantially longer period shielded from RA signalling than the early migrating cells that generate the rostral IM (Fig. 5A).

FGFs are not only involved in chemotaxis but also in the differentiation of the primitive streak into the mesoderm. FGFs can induce mesoderm formation from the animal cap of *Xenopus*, chick pregastrula epiblast and human primitive streak (Amaya et al., 1993; Yatskievych et al., 1997; Takasato et al., 2014a). During cell migration, the streak cells differentiate into mesoderm via an epithelial to mesenchymal transition (EMT) that requires FGFR1 expression (Ciruna et al., 1997). In *Fgfr1* mutant mice, EMT is blocked by the lack of *Snai1* (snail family zinc finger 1), causing the cells to fail to migrate from the streak (Ciruna and Rossant, 2001). FGF signalling is inhibited by the RA pathway (and vice versa), and this mutual inhibition controls A-P patterning and mesodermal differentiation during axis extension (del Corral et al., 2003; Dorey and Amaya, 2010). Indeed, a recent study demonstrated that RA represses the transcription of *Fgf8* (Kumar and Duester, 2014), whereas *Cyp26a1* expression is not affected by the lack of *Fgfr1* (Wahl et al., 2007; Martin and Kimelman, 2010).

Importantly, an FGF8-responding domain expressing *Fgf8* target genes such as *Etv4*/*Pea3* and *Etv5*/*Erm* exists slightly rostrally to the Cyp26a1-expressing domain in both mouse and zebrafish (Wahl et al., 2007; Martin and Kimelman, 2010). This suggests the presence of three distinct mesodermal domains along A-P axis from the caudal end (domains i, ii and iii in Fig. 5A): an FGF8-responding domain; a domain responding to both RA and FGF8; and a RA-responding domain. The third domain is likely to respond to other FGFs as it does express *Fgfr1* (Wahl et al., 2007). Such FGFs may promote mesodermal identity and survival in migrating cells. For example, *Fgf9* and *Fgf20* are necessary for the acquisition of MM identity from E10.5 (Barak et al., 2012). An understanding of both the mechanisms of fate specification and the regulation of these fate decisions will be crucial to recapitulate such events *in vitro*.

The regulation of mesoderm patterning along the medio-lateral axis

In addition to the A-P patterning of the trunk mesoderm, patterning along the medio-lateral (M-L) axis is also required for the specification of the PM, IM and LPM (Fig. 5B). We have described previously the evidence indicating that the PM originates from the anterior PSM, whereas the LPM is derived from the posterior PSM (James and Schultheiss, 2003; Sweetman et al., 2008). This suggests that the IM originates from an intermediary region of the streak, localized between the other two (asterisk in Fig. 3B). M-L patterning is also thought to be controlled via regionalized BMP signalling (via ALK3/BMPR1A- or ALK6/BMPR1B-mediated signalling): high levels of BMP4 specify the LPM, low levels of BMP signalling are required for the formation of the IM, and noggin-mediated BMP4 antagonism is necessary for PM specification (Barak et al., 2005; Wijgerde et al., 2005; James and Schultheiss, 2005) (Fig. 5B). In the embryonic trunk, the BMP antagonist noggin (NOG), is secreted from the spinal cord, notochord and dorsal lip of the PM to protect it from the BMP4 secreted by the LPM. Hence, the PM in *Nog* mutant mice is reduced in size (Wijgerde et al., 2005). Furthermore, explant cultures of chicken anterior or posterior streak, with the addition of BMP2 or NOG, respectively, demonstrated that M-L cell fates are interchangeable (James and Schultheiss, 2005). During the development of the IM, a low level of BMP signalling is required for the formation of the nephric duct (Obara-Ishihara et al., 1999). In addition to BMP, nodal/activin (ALK4/ACVR1B-mediated signalling) expressed by the LPM is essential for IM specification as its overexpression expands the IM domain in the chick (Fleming et al., 2013). Nodal, which is secreted by the LPM, is antagonized by cerberus 1, which is secreted from the PM, creating a gradient of nodal signalling along M-L axis (Biben et al., 1998). Hence, M-L cell fates are determined by cell positions within M-L morphogen gradients after the cell migration from the PSM. That cell position, however, initially results from A-P positional information in the PSM.

The MM and the UB originate from distinct regions of the IM

Having defined the signals that determine to which mesoderm subtype (PM, IM and LPM) a given PSM-derived cell might contribute, we can revisit what is required to make the different components of a metanephros from the IM. Although both the UB and MM are derived from the IM, there appear to be distinct temporal and spatial distinctions between these two populations.

Regarding the MM, *T* lineage-tracing studies showed that both the metanephric and the mesonephric mesenchyme (NM between the fore and hindlimbs) were marked after an E8.5 tamoxifen injection (Taguchi et al., 2014). This raises two possibilities: (1) the progenitors of the mesonephric mesenchyme migrate from the PSM after E8.5, but earlier than the MM progenitors (early divergence); or (2) PSM daughter cells that migrate after E8.5 give rise to a common mesenchymal field that subsequently separates to form mesonephric and metanephric mesenchyme (late divergence). The significant congruence in gene expression during the development of both regions (Georgas et al., 2011), with perhaps the exception of *Hox11* paralogue expression (Wellik et al., 2002; Challen et al., 2004), suggests the latter, as does recent *Eya1* lineage tracing. *Eya1* (eyes absent 1) is a transcription factor first observed at around E8.5 in the caudal IM (Sajithlal et al., 2005) and essential for the formation of the MM, prior to UB invasion (Fig. 6). Another transcription factor, *Lhx1* (LIM homeobox 1), is initially expressed in the rostral IM at E8.5. By E9, *Lhx1* expression is restricted to the nephric duct, whereas the *Eya1* domain in the IM extends caudally alongside the *Lhx1*$^{+}$ nephric duct (Fig. 6). Lineage tracing of *Eya1*$^{+}$ cells (*Eya1-CreER*×*R26R-LacZ* mice) showed that whereas E8.5-8.75 tamoxifen injection marked *Eya1*$^{+}$ caudal IM, those cells did not give rise to ND, collecting ducts, rostral mesonephric tubules or kidney stroma cells (Xu et al., 2014). These cells did, however, give rise to caudal mesonephric tubules, to MM and to MM derivatives in the metanephros (Xu et al., 2014) (Fig. 6).

Obvious differences in morphology and provenance between rostral and caudal mesonephros further support the possibility of two early restricted IM progenitors. Indeed, the mesonephric tubules forming in the rostral mesonephros connect to the nephric duct from early in meso-nephrogenesis (Georgas et al., 2011) and are derived from the *Hoxb7*$^{+}$ ND (Sainio et al., 1997; Kobayashi et al., 2005a), whereas the caudal mesonephric tubules are derived from the NM (Kobayashi et al., 2005a). However, while displaying gene expression similar to early nephrons in the metanephros (Georgas et al., 2011), they do not connect to the nephric duct (Fig. 6). Indeed, *Wt1* (Wilms' tumour 1) mutant mice only develop the rostral mesonephros but fail to form the caudal mesonephros or metanephros (Kreidberg et al., 1993; Sainio et al., 1997), indicating a lineage boundary between IM-forming rostral (pronephric and the rostral mesonephric domain) and caudal (caudal mesonephric and metanephric) nephrogenic mesenchyme.

This concept of a lineage boundary between rostral (early) and caudal (late) IM is also supported by our understanding of nephric duct formation. *Gata3*, a zinc-finger transcription factor (Patient and McGhee, 2002), is expressed in the ND from its induction (Fig. 6). *Gata3* continues to be expressed in the elongating nephric duct and

Development (2015) 142, 1937-1947 doi:10.1242/dev.104802

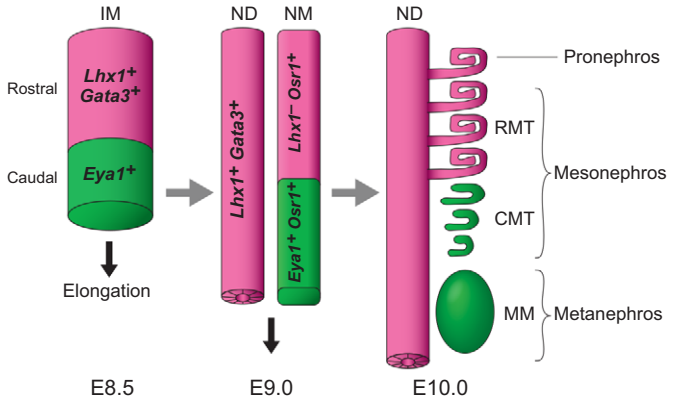

Fig. 6. Development of the rostral and caudal intermediate mesoderm. This diagram illustrates a fate map of the rostral IM (pink) and caudal IM (green) at three timepoints (E8.5, E9.0 and E10) of mouse embryogenesis.+ and – indicate the presence or the absence of the indicated gene transcript in that domain. CMT, caudal mesonephric tubules; IM, intermediate mesoderm; MM, metanephric mesenchyme; ND, nephric duct/Wolffian duct; NM, nephrogenic mesenchyme; RMT, rostral mesonephric tubules.

the derivative UB, both before the UB reaches the mesenchyme and during subsequent UB branching (George et al., 1994; Labastie et al., 1995; Sheng and Stern, 1999). By E8.5, a *Gata3*$^+$ IM develops into the rostral IM of the embryo trunk. With surprising speed, this *Gata3*$^+$ nephric duct completes elongation to the cloaca by E10 (Grote et al., 2006). Time-lapse imaging of this process using *Hoxb7*-GFP mice shows that the nephric duct elongates caudally via migration of GFP$^+$ cells (Chi et al., 2009). *Gata3* itself is necessary for this caudal elongation, as this is halted from the mesonephric region onwards in *Gata3* mutant mice (Grote et al., 2006). However, a *Pax2*$^+$*Wt1*$^+$ MM still arises from the caudal trunk independently of this blockage. Lineage studies based on *T* and *Eya1* (Taguchi et al., 2014; Xu et al., 2014) are consistent with the idea that the UB is derived from the rostral IM. However, their conclusions regarding the origin of the MM differ. Having proposed that the MM is derived from *Eya1*$^+$ caudal IM arising from E8.5, *in situ* hybridization analysis of *T* mRNA at E8.5 does not show the expression of *T* in the caudal IM at that stage (Galceran et al., 2001). This may result from a lack of *in situ* hybridization resolution at this timepoint or from the fact that tamoxifen injected at E8.5 may perdure for 24 h, facilitating the tagging of *Eya1*$^+$ caudal nephrogenic mesenchyme cells derived from *T*$^+$ PSM at E8.5 as late as E9.0-9.5. However, all these studies suggest that while the UB and the MM do originate from one common source, the primitive streak, there are distinct origins for the nephric duct/UB and the MM (Fig. 6). This has implications for approaches to kidney regeneration.

Implications for recreating the kidney *in vitro*

The isolation of the first human embryonic stem cells (hESCs) (Thomson et al., 1998) opened up the possibility for *in vitro* differentiation of hESCs into specific cellular tissues, and hence the prospect of cellular therapy and bioengineering. Furthermore, the advent of iPSCs circumvented the ethical dilemma surrounding hESCs, as well as providing the potential to recreate cells for autologous applications. Protocols for directed differentiation of hPSCs have now been developed for many cell types. In the kidney field, early attempts at generating specific kidney tissues began using mouse ESCs (Yamamoto et al., 2006; Steenhard et al., 2005; Kim and Dressler, 2005; Kobayashi et al., 2005b; Bruce et al., 2007; Vigneau et al., 2007; Morizane et al., 2009; Mae et al., 2010; Ren et al., 2010; Nishikawa et al., 2012; reviewed by Takasato et al., 2014b). Early attempts at directed differentiation of hPSCs into kidney tissues, focused on identification of specific endpoints, including podocytes (Song et al., 2012) and proximal tubules (Narayanan et al., 2013). In neither of these studies was there a comprehensive evaluation of intervening steps. The field as a whole strongly embraced the concept of stepwise differentiation of hPSCs through recognizable intermediate stages of embryogenesis. This strategy has now been adopted by a number of groups studying kidney development (Mae et al., 2013; Xia et al., 2013; Lam et al., 2014; Takasato et al., 2014a; Taguchi et al., 2014) who have used all of the growth factors described above as influencing primitive streak formation (RA, activin A, FGF2, WNT3A), A-P mesodermal patterning (RA, FGF2/9, WNT3A/5A), M-L mesodermal patterning (BMP4, activin A, FGFs), nephric duct identity (RA, activin A), MM fate (WNTs, BMP7, FGF2/9) and survival (FGF2/9, BMP2/7). We will focus on three such studies (Xia et al., 2013; Taguchi et al., 2014; Takasato et al., 2014a) (Fig. 7).

Xia et al. (2013) reported a protocol to generate UB progenitor-like epithelial cells from hPSCs (Fig. 7, upper panel). This protocol requires only 4 days of monolayer culture and begins with the induction of a *T*$^+$ mesoderm via the addition of BMP4 and FGF2. Subsequent addition of a combination of RA, activin A and BMP2 resulted in the expression of *OSR1* (odd skipped-related 1), *PAX2* (paired box 2), *GATA3*, *PAX8* and *LHX1*, all genes expressed in the developing nephric duct and UB, as assessed by qPCR. When this population was co-cultured with dissociated total embryonic mouse kidney, human cells were seen to integrate into and contribute to a CK8$^+$ (keratin 8, *KRT8*) epithelium with these cells surrounded by mouse collecting duct cells. This suggests that this protocol can generate UB-like progenitors. However, differentiated hPSCs were not able to act as nephrogenic mesenchyme or form nephrons when cultured with isolated murine UBs.

In contrast to Xia et al. (2013), Taguchi and colleagues (2014) approached the challenge using mouse ESCs, and then transferred the approach to hPSCs, generating metanephric mesenchyme but not nephric duct/UB (Fig. 7, middle). Their protocol begins with BMP4-induced formation of embryoid bodies that are then exposed to activin A/FGF2 to form epiblast. A transition from epiblast to nascent mesoderm (PSM), marked by the expression of *CDX2* (caudal type homeobox 2) and continued expression of *T*, was induced with the addition of BMP4 and the WNT agonist CHIR99201. The transition from this *T*$^+$*CDX2*$^+$ nascent mesoderm to (caudal) IM (*OSR1*$^+$*PAX2*$^+$ but *T*$^-$ *CDX2*$^-$) was observed after the addition of activin A/BMP4/RA/CHIR99201. This caudal IM population was able to form MM after the addition of FGF9 and continued low WNT agonist activity, consistent with the literature (Karner et al., 2011; Barak et al., 2012). Furthermore, this MM was able to form nephron structures via co-culture with the spinal cord, which mimics UB-induced nephron formation. The nephrons formed have Bowman's capsules containing avascular glomeruli that express markers of podocyte differentiation and are attached to elongating renal tubule segments. When generated using mouse ESCs, the resulting structures were placed under the kidney capsule of recipient animals where the glomeruli vascularised, presumably via the incorporation of host-derived vascular progenitors. Hence, this study represents the best evidence to date of the generation of nephron components from pluripotent stem cells.

In our own studies (Takasato et al., 2014a), we employed a monolayer culture of a MIXL1-GFP reporter hESC line, which is indicative of primitive streak identity (Davis et al., 2008), in fully

Development (2015) 142, 1937-1947 doi:10.1242/dev.104802

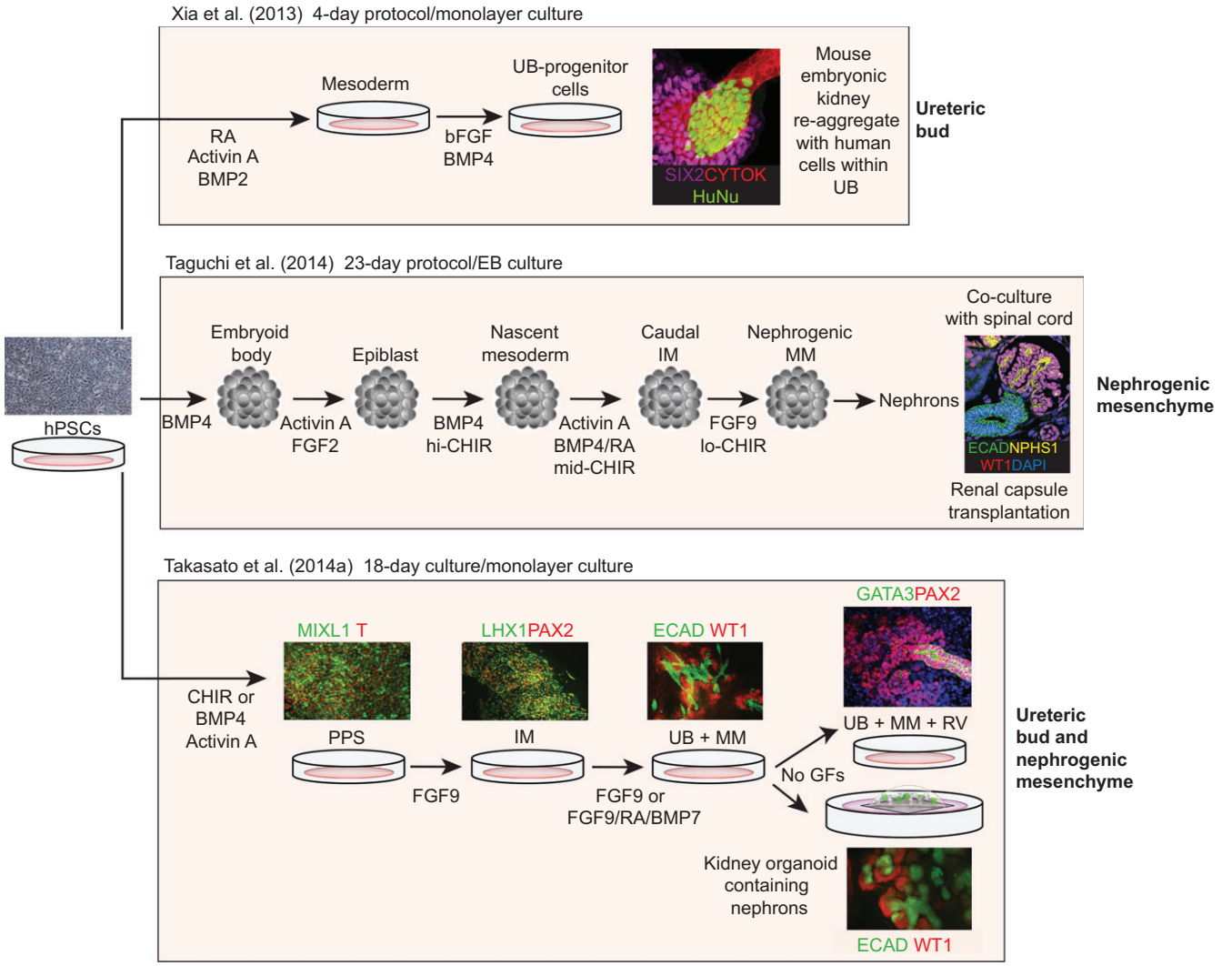

Fig. 7. Stepwise differentiation of hPSCs to kidney endpoints: a comparison of three approaches. The stepwise differentiation protocols presented by Xia et al. (2013), Taguchi et al. (2014) and Takasato et al. (2014a) illustrating the culture method (monolayer versus EB), the growth factors, the identified intermediate and the final outcomes. All three commenced with undifferentiated human pluripotent stem cells (hPSCs). Xia et al. (2013) reported a monolayer-based culture protocol generating ureteric bud-progenitor cells able to contribute to the collecting duct when re-aggregated with embryonic mouse kidney. Taguchi et al. (2014) reported an embryoid body-based protocol that generated nephrogenic mesenchyme capable of differentiating into segmented nephrons, including nephrosis 1 (NPHS1)$^{+}$WT1^{+} glomeruli, *in vitro*. When generated from mESC, these glomeruli vascularised when transplanted into a host animal. Takasato et al. (2014a) employed a monolayer culture-based protocol that generated cells able to initiate nephrogenesis on a dish via reciprocal interaction between UB and MM. These cultures, when re-aggregated as human cells alone, formed kidney organoids containing both collecting duct and nephrons. Image relating to Taguchi et al. (2014) provided by Professor Ryuichi Nischinakamura and Dr Atsuhiro Taguchi. Image relating to Xia et al. (2013) provided by Professor Juan Carlos Izpisua Belmonte. CHIR, WNT agonist CHIR99201; EB, embryoid body; GF, growth factor; IM, intermediate mesoderm; MM, metanephric mesenchyme; PPS, posterior primitive streak; RV, renal vesicle; UB, ureteric bud.

defined medium (Ng et al., 2008) (Fig. 7, bottom). The *MIXL1* (Mix1 homeobox-like 1) reporter cell line enabled the monitoring of the first stage of differentiation, the induction of primitive streak identity, which was achieved via the addition of either CHIR99021 or a combination of high BMP4/low activin A, resulting in 90-95% GFP^{+} cells. Beyond this stage, if cells were allowed to spontaneously differentiate, a population of *OSR1*$^{+}$ mesenchyme arose. This population was *PAX2*$^{-}$*LHX1*$^{-}$ but positive for *FOXF1* (forkhead box F1) expression, suggesting that it was more likely to represent LPM than IM. This indicates that the starting population of primitive streak was likely to be posterior primitive streak (PPS) and hence more likely to form mesoderm than endoderm. To specify the IM from PPS, we found that the addition of FGF9 or FGF2, but not FGF8, robustly induced *PAX2* and *LHX1* but suppressed the expression of *FOXF1*. This finding indicates that FGF signalling other than the FGF/MAPK regulates M-L patterning of the trunk mesoderm. Furthermore, this IM specification was suppressed by the addition of BMP4, suggesting a possible interaction between FGFs and BMP4 in the context of M-L patterning. Such a role for FGF signalling has not previously been proposed based on conventional knockout mouse studies, possibly due to redundancy between FGF family members. Indeed, FGF9 or FGF2 mutant mice were not reported as showing any defects in IM development (Dono et al., 1998; Ortega et al., 1998; Barak et al., 2012). The final stage of differentiation was achieved using a combination of FGF9, RA and BMP7. After ~4 days, a proportion of the *PAX2*$^{+}$ population appeared to undergo MET to form *GATA3*$^{+}$*PAX2*$^{+}$*ECAD*$^{+}$ (cadherin 1, *CDH1*) *Dolichos biflorus* (DBA)-stained tubules, suggestive of nephric duct/UB identity. This tissue was surrounded by a *SIX2*$^{+}$*WT1*$^{+}$*HOXD11*$^{+}$ mesenchyme,

Development (2015) 142, 1937-1947 doi:10.1242/dev.104802

suggestive of MM. QPCR performed during the differentiation timecourse, coupled with IF for a panel of nephric duct/UB and MM markers, confirmed the simultaneous formation of both key compartments of the developing kidney. Similar results were obtained using FGF9 alone during this stage of differentiation. This phenomenon is consistent with *Fgfr2* expression in the nephric duct in the mouse embryo (Grote et al., 2008). In addition, although not essential, RA appeared to enhance the differentiation of $PAX2^+GATA3^+$ nephric duct cells, as might be anticipated from the role of RA in A-P patterning described above. The reintroduction of these hPSC-derived populations into embryonic mouse kidney showed evidence of their contribution to both UB and nephrogenic mesenchyme compartments. Furthermore, by 18 days of culture, cells reorganized to form 3D structures comprising a ureteric epithelium surrounded by a mesenchyme that subsequently underwent MET to form $JAG1^+CDH6^+$ (jagged 1/cadherin 6) renal vesicles, the first stage of nephron formation. Together, these studies provide promising evidence of the potential to recreate kidney organogenesis *in vitro* from pluripotent sources.

Reconciling the *in vitro* reconstitution of kidney tissues with our understanding of kidney development

Takasato et al. (2014a) is the only report to date of the simultaneous differentiation of both MM and UB populations. At face value, the observations of Taguchi et al. (2014) suggest that this would not be possible. How can we reconcile these observations with the embryology? In order to avoid the generation of nephric duct/UB, Taguchi et al. (2014) selected for conditions that would avoid the generation of an early $OSR1^+$ population, instead generating a more caudal T^+CDX2^+ population first. As discussed above, temporal and spatial patterning of the IM is controlled by gradients of RA, FGF and WNT signalling. It is of interest, therefore, that the key differences between Taguchi et al. (2014) and Takasato et al. (2014a) lie in the use and timing of WNT agonist and FGF9. Taguchi et al. (2014) directed the differentiation of T^+ nascent mesoderm into IM via the addition of activin A, BMP4, RA and WNT agonist. Unlike all other studies, Takasato specified PPS into IM in the presence of FGF9 and not via the addition of BMP or activin/nodal signalling. This gave rise to a strongly $PAX2^+LHX1^+OSR1^+$ rostral IM population, within which there is a scattered $PAX2^+LHX1^-$ subpopulation that represents $LHX1^-$ caudal IM. The fact that cultures were not fractionated to separate these two populations appears to have facilitated a capacity to form both the MM and the UB. Indeed, the presence of the RA may assist in the onward differentiation of the ureteric component. As discussed above, while IM specification can be induced by FGF9 and nephric duct outgrowth is also regulated by FGF9 (Takasato et al., 2014a), MM specification and maintenance also require FGF9 (Barak et al., 2012), implying that common inducing factors supported both lineages *in vitro*.

Another key difference between the two studies was the consistent presence of a WNT agonist, from presumptive epiblast stage through to the formation of nephrons, in the protocol of Taguchi et al. (2014). It is possible that having this WNT signal present in a constant fashion was sufficient to mimic the PSM environment sufficiently to prevent an early induction of nephric duct. The addition of WNT agonist through this developmental timecourse was absent from Xia et al. (2013), possibly explaining the total lack of MM or MM derivatives in that protocol. Takasato et al. (2014a) did not add WNT agonists after the initial induction of posterior primitive streak. Hence, the presence of MM can only be attributed to the support of FGF9±BMP7.

Conclusions and perspectives

The directed differentiation of human PSCs into kidney tissues is an exciting advance that has drawn on knowledge from mouse development. Hence, murine developmental morphogenesis has guided human regeneration. In this Review, we have attempted to reconcile retrospectively what has been observed upon the *in vitro* differentiation of hPSCs to kidney with the current understanding of mouse embryogenesis. We conclude that the rostral or early intermediate mesoderm gives rise to UB, pronephros and rostral mesonephros (including all cranial mesonephric ducts), while the caudal or later intermediate mesoderm gives rise to the caudal mesonephros (including all caudal mesonephric ducts) and the MM. This is not inconsistent with the view of Taguchi et al. (2014); however, the earlier common origin of both rostral and caudal IM, as extensively reviewed here, may explain the observations of simultaneous generation of UB and MM-derived structures derived *in vitro*, as seen by Takasato et al. (2014a).

Although the anatomical similarity between mouse and human in early development appears to be strong, we cannot be sure that mouse and human are the same at the level of gene expression or lineage relationships. Furthermore, lineage tracing in humans is impossible, for obvious reasons, and there has been next to no expression profiling of these early stages of metanephric development in human. To date, two studies were carried out at stages where nephrogenesis is already established or close to completion, providing no information about the concordance between mouse and human with respect to early patterning events (Cutcliffe et al., 2005; Karlsson et al., 2014). In addition, both of these studies involved profiling of whole organs and therefore represent very complex samples in which all cell types are present. This makes the resolution of developmental gene expression in any given cellular compartment impossible to dissect. However, although the study of early human kidney development remains inaccessible directly, there certainly does appear to be sufficient evidence for the successful generation of embryonic kidney cell populations from hPSCs. This provides the first opportunity for expression analysis of at least endpoint populations to begin to examine similarities with mouse and identify distinct genetic regulation in human development. Several crucial questions remain unanswered. Are the populations being generated *in vitro* equivalent to those present in the human foetal kidney or are they by-products of the *in vitro* process? If they genuinely reflect normal human development, what stage of development is, or can be, reached *in vitro*? Can directed differentiation of human PSCs act as an accurate surrogate of early human development to better interrogate the effect of environmental/gestational insult on development? Can hPSC-derived kidney organoids be used as disease models or drug screening tools for the development of new treatments? If the kidney populations generated *in vitro* indeed represent a developmental step in human kidney morphogenesis, we will have come full circle with regeneration teaching us about development.

Acknowledgements

M.L. is a Senior Principal Research Fellow of the National Health and Medical Research Council of Australia). We thank Professor Ryuichi Nishinakamura, Dr Atsuhiro Taguchi, Professor Juan Carlos Izpisua Belmonte and Professor Dylan Sweetman for providing figures and for permission to reproduce their data.

Competing interests

The authors declare no competing or financial interests.

Funding

This work is supported by the Australian Research Council [Stem Cells Australia SRI110001002, DP130102939] and the National Health and Medical Research Council Australia [APP1041277]. M.L. receives research support from Organovo.

References

Abu-Abed, S., Dollé, P., Metzger, D., Beckett, B., Chambon, P. and Petkovich, M. (2001). The retinoic acid-metabolizing enzyme, CYP26A1, is essential for normal hindbrain patterning, vertebral identity, and development of posterior structures. *Genes Dev.* **15**, 226-240.

Amaya, E., Stein, P. A., Musci, T. J. and Kirschner, M. W. (1993). FGF signalling in the early specification of mesoderm in Xenopus. *Development* **118**, 477-487.

Anderson, M. J., Naiche, L. A., Wilson, C. P., Elder, C., Swing, D. A. and Lewandoski, M. (2013). TCreERT2, a transgenic mouse line for temporal control of Cre-mediated recombination in lineages emerging from the primitive streak or tail bud. *PLoS ONE* **8**, e62479.

Attia, L., Yelin, R. and Schultheiss, T. M. (2012). Analysis of nephric duct specification in the avian embryo. *Development* **139**, 4143-4151.

Barak, H., Rosenfelder, L., Schultheiss, T. M. and Reshef, R. (2005). Cell fate specification along the anterior-posterior axis of the intermediate mesoderm. *Dev. Dyn.* **232**, 901-914.

Barak, H., Huh, S.-H., Chen, S., Jeanpierre, C., Martinovic, J., Parisot, M., Bole-Feysot, C., Nitschké, P., Salomon, R., Antignac, C. et al. (2012). FGF9 and FGF20 maintain the stemness of nephron progenitors in mice and man. *Dev. Cell* **22**, 1191-1207.

Bénazéraf, B., Francois, P., Baker, R. E., Denans, N., Little, C. D. and Pourquié, O. (2010). A random cell motility gradient downstream of FGF controls elongation of an amniote embryo. *Nature* **466**, 248-252.

Bertram, J. F., Douglas-Denton, R. N., Diouf, B., Hughson, M. D. and Hoy, W. E. (2011). Human nephron number: implications for health and disease. *Pediatr. Nephrol.* **26**, 1529-1533.

Biben, C., Stanley, E., Fabri, L., Kotecha, S., Rhinn, M., Drinkwater, C., Lah, M., Wang, C.-C., Nash, A., Hilton, D. et al. (1998). Murine cerberus homologue mCer-1: a candidate anterior patterning molecule. *Dev. Biol.* **194**, 135-151.

Boulet, A. M. and Capecchi, M. R. (2012). Signaling by FGF4 and FGF8 is required for axial elongation of the mouse embryo. *Dev. Biol.* **371**, 235-245.

Bruce, S. J., Rea, R. W., Steptoe, A. L., Busslinger, M., Bertram, J. F. and Perkins, A. C. (2007). In vitro differentiation of murine embryonic stem cells toward a renal lineage. *Differentiation* **75**, 337-349.

Carroll, T. J., Park, J.-S., Hayashi, S., Majumdar, A. and McMahon, A. P. (2005). Wnt9b plays a central role in the regulation of mesenchymal to epithelial transitions underlying organogenesis of the mammalian urogenital system. *Dev. Cell* **9**, 283-292.

Challen, G. A., Martinez, G., Davis, M. J., Taylor, D. F., Crowe, M., Teasdale, R. D., Grimmond, S. M. and Little, M. H. (2004). Identifying the molecular phenotype of renal progenitor cells. *J. Am. Soc. Nephrol.* **15**, 2344-2357.

Chi, X., Michos, O., Shakya, R., Riccio, P., Enomoto, H., Licht, J. D., Asai, N., Takahashi, M., Ohgami, N., Kato, M. et al. (2009). Ret-dependent cell rearrangements in the Wolffian duct epithelium initiate ureteric bud morphogenesis. *Dev. Cell* **17**, 199-209.

Ciruna, B. and Rossant, J. (2001). FGF signaling regulates mesoderm cell fate specification and morphogenetic movement at the primitive streak. *Dev. Cell* **1**, 37-49.

Ciruna, B. G., Schwartz, L., Harpal, K., Yamaguchi, T. P. and Rossant, J. (1997). Chimeric analysis of fibroblast growth factor receptor-1 (Fgfr1) function: a role for FGFR1 in morphogenetic movement through the primitive streak. *Development* **124**, 2829-2841.

Cutcliffe, C., Kersey, D., Huang, C.-C., Zeng, Y., Walterhouse, D. and Perlman, E. J.; **for the Renal Tumor Committee of the Children's Oncology Group** (2005). Clear cell sarcoma of the kidney: up-regulation of neural markers with activation of the sonic hedgehog and Akt pathways. *Clin. Cancer Res.* **11**, 7986-7994.

Davis, R. P., Ng, E. S., Costa, M., Mossman, A. K., Sourris, K., Elefanty, A. G. and Stanley, E. G. (2008). Targeting a GFP reporter gene to the MIXL1 locus of human embryonic stem cells identifies human primitive streak-like cells and enables isolation of primitive hematopoietic precursors. *Blood* **111**, 1876-1884.

del Corral, R. D., Olivera-Martinez, I., Goriely, A., Gale, E., Maden, M. and Storey, K. (2003). Opposing FGF and retinoid pathways control ventral neural pattern, neuronal differentiation, and segmentation during body axis extension. *Neuron* **40**, 65-79.

Delfini, M.-C., Dubrulle, J., Malapert, P., Chal, J. and Pourquié, O. (2005). Control of the segmentation process by graded MAPK/ERK activation in the chick embryo. *Proc. Natl. Acad. Sci. USA* **102**, 11343-11348.

Deschamps, J. and van Nes, J. (2005). Developmental regulation of the Hox genes during axial morphogenesis in the mouse. *Development* **132**, 2931-2942.

Dono, R., Texido, G., Dussel, R., Ehmke, H. and Zeller, R. (1998). Impaired cerebral cortex development and blood pressure regulation in FGF-2-deficient mice. *EMBO J.* **17**, 4213-4225.

Dorey, K. and Amaya, E. (2010). FGF signalling: diverse roles during early vertebrate embryogenesis. *Development* **137**, 3731-3742.

Dubrulle, J., McGrew, M. J. and Pourquié, O. (2001). FGF signaling controls somite boundary position and regulates segmentation clock control of spatiotemporal hox gene activation. *Cell* **106**, 219-232.

Duester, G. (2008). Retinoic acid synthesis and signaling during early organogenesis. *Cell* **134**, 921-931.

Dunty, W. C., Biris, K. K., Chalamalasetty, R. B., Taketo, M. M., Lewandoski, M. and Yamaguchi, T. P. (2008). Wnt3a/beta-catenin signaling controls posterior body development by coordinating mesoderm formation and segmentation. *Development* **135**, 85-94.

Fleming, B. M., Yelin, R., James, R. G. and Schultheiss, T. M. (2013). A role for Vg1/Nodal signaling in specification of the intermediate mesoderm. *Development* **140**, 1819-1829.

Forlani, S., Lawson, K. A. and Deschamps, J. (2003). Acquisition of Hox codes during gastrulation and axial elongation in the mouse embryo. *Development* **130**, 3807-3819.

Galceran, J., Hsu, S.-C. and Grosschedl, R. (2001). Rescue of a Wnt mutation by an activated form of LEF-1: regulation of maintenance but not initiation of Brachyury expression. *Proc. Natl. Acad. Sci. USA* **98**, 8668-8673.

Georgas, K. M., Chiu, H. S., Lesieur, E., Rumballe, B. A. and Little, M. H. (2011). Expression of metanephric nephron-patterning genes in differentiating mesonephric tubules. *Dev. Dyn.* **240**, 1600-1612.

George, K. M., Leonard, M. W., Roth, M. E., Lieuw, K. H., Kioussis, D., Grosveld, F. and Engel, J. D. (1994). Embryonic expression and cloning of the murine GATA-3 gene. *Development* **120**, 2673-2686.

Grote, D., Souabni, A., Busslinger, M. and Bouchard, M. (2006). Pax2/8-regulated Gata3 expression is necessary for morphogenesis and guidance of the nephric duct in the developing kidney. *Development* **133**, 53-61.

Grote, D., Boualia, S. K., Souabni, A., Merkel, C., Chi, X., Costantini, F., Carroll, T. and Bouchard, M. (2008). Gata3 acts downstream of beta-catenin signaling to prevent ectopic metanephric kidney induction. *PLoS Genet.* **4**, e1000316.

Hartman, H. A., Lai, H. L. and Patterson, L. T. (2007). Cessation of renal morphogenesis in mice. *Dev. Biol.* **310**, 379-387.

Hinchliffe, S. A., Sargent, P. H., Howard, C. V., Chan, Y. F. and van Velzen, D. (1991). Human intrauterine renal growth expressed in absolute number of glomeruli assessed by the disector method and Cavalieri principle. *Lab. Invest.* **64**, 777-784.

Horikawa, K., Radice, G., Takeichi, M. and Chisaka, O. (1999). Adhesive subdivisions intrinsic to the epithelial somites. *Dev. Biol.* **215**, 182-189.

James, R. G. and Schultheiss, T. M. (2003). Patterning of the avian intermediate mesoderm by lateral plate and axial tissues. *Dev. Biol.* **253**, 109-124.

James, R. G. and Schultheiss, T. M. (2005). Bmp signaling promotes intermediate mesoderm gene expression in a dose-dependent, cell-autonomous and translation-dependent manner. *Dev. Biol.* **288**, 113-125.

Karlsson, J., Holmquist Mengelbier, L., Ciornei, C. D., Naranjo, A., O'Sullivan, M. J. and Gisselsson, D. (2014). Clear cell sarcoma of the kidney demonstrates an embryonic signature indicative of a primitive nephrogenic origin. *Genes Chromosom. Cancer* **53**, 381-391.

Karner, C. M., Das, A., Ma, Z., Self, M., Chen, C., Lum, L., Oliver, G. and Carroll, T. J. (2011). Canonical Wnt9b signaling balances progenitor cell expansion and differentiation during kidney development. *Development* **138**, 1247-1257.

Kim, D. and Dressler, G. R. (2005). Nephrogenic factors promote differentiation of mouse embryonic stem cells into renal epithelia. *J. Am. Soc. Nephrol.* **16**, 3527-3534.

Kinder, S. J., Tsang, T. E., Quinlan, G. A., Hadjantonakis, A. K., Nagy, A. and Tam, P. P. (1999). The orderly allocation of mesodermal cells to the extraembryonic structures and the anteroposterior axis during gastrulation of the mouse embryo. *Development* **126**, 4691-4701.

Kinder, S. J., Tsang, T. E., Wakamiya, M., Sasaki, H., Behringer, R. R., Nagy, A. and Tam, P. P. (2001). The organizer of the mouse gastrula is composed of a dynamic population of progenitor cells for the axial mesoderm. *Development* **128**, 3623-3634.

Kmita, M. and Duboule, D. (2003). Organizing axes in time and space; 25 years of colinear tinkering. *Science* **301**, 331-333.

Kobayashi, A., Kwan, K.-M., Carroll, T. J., McMahon, A. P., Mendelsohn, C. L. and Behringer, R. R. (2005a). Distinct and sequential tissue-specific activities of the LIM-class homeobox gene Lim1 for tubular morphogenesis during kidney development. *Development* **132**, 2809-2823.

Kobayashi, T., Tanaka, H., Kuwana, H., Inoshita, S., Teraoka, H., Sasaki, S. and Terada, Y. (2005b). Wnt4-transformed mouse embryonic stem cells differentiate into renal tubular cells. *Biochem. Biophys. Res. Commun.* **336**, 585-595.

Kreidberg, J. A., Sariola, H., Loring, J. M., Maeda, M., Pelletier, J., Housman, D. and Jaenisch, R. (1993). WT-1 is required for early kidney development. *Cell* **74**, 679-691.

Kress, C., Vogels, R., De Graaff, W., Bonnerot, C., Meijlink, F., Nicolas, J. F. and Deschamps, J. (1990). Hox-2.3 upstream sequences mediate lacZ expression in intermediate mesoderm derivatives of transgenic mice. *Development* **109**, 775-786.

Kumar, S. and Duester, G. (2014). Retinoic acid controls body axis extension by directly repressing Fgf8 transcription. *Development* **141**, 2972-2977.

Labastie, M.-C., Catala, M., Gregoire, J.-M. and Peault, B. (1995). The GATA-3 gene is expressed during human kidney embryogenesis. *Kidney Int.* **47**, 1597-1603.

Lam, A. Q., Freedman, B. S., Morizane, R., Lerou, P. H., Valerius, M. T. and Bonventre, J. V. (2014). Rapid and efficient differentiation of human pluripotent

stem cells into intermediate mesoderm that forms tubules expressing kidney proximal tubular markers. *J. Am. Soc. Nephrol.* **25**, 1211-1225.
Little, M. H. and McMahon, A. P. (2012). Mammalian kidney development: principles, progress, and projections. *Cold Spring Harb. Perspect. Biol.* **4**, a008300.
Little, M. H., Brennan, J., Georgas, K., Davies, J. A., Davidson, D. R., Baldock, R. A., Beverdam, A., Bertram, J. F., Capel, B., Chiu, H. S. et al. (2007). A high-resolution anatomical ontology of the developing murine genitourinary tract. *Gene Expr. Patterns.* **7**, 680-699.
Mae, S.-I., Shirasawa, S., Yoshie, S., Sato, F., Kanoh, Y., Ichikawa, H., Yokoyama, T., Yue, F., Tomotsune, D. and Sasaki, K. (2010). Combination of small molecules enhances differentiation of mouse embryonic stem cells into intermediate mesoderm through BMP7-positive cells. *Biochem. Biophys. Res. Commun.* **393**, 877-882.
Mae, S.-I., Shono, A., Shiota, F., Yasuno, T., Kajiwara, M., Gotoda-Nishimura, N., Arai, S., Sato-Otubo, A., Toyoda, T., Takahashi, K. et al. (2013). Monitoring and robust induction of nephrogenic intermediate mesoderm from human pluripotent stem cells. *Nat. Commun.* **4**, 1367.
Martin, B. L. and Kimelman, D. (2010). Brachyury establishes the embryonic mesodermal progenitor niche. *Genes Dev.* **24**, 2778-2783.
Merlet-Bénichou, C., Gilbert, T., Vilar, J., Moreau, E., Freund, N. and Lelièvre-Pégorier, M. (1999). Nephron number: variability is the rule. Causes and consequences. *Lab Invest.* **79**, 515-527.
Morizane, R., Monkawa, T. and Itoh, H. (2009). Differentiation of murine embryonic stem and induced pluripotent stem cells to renal lineage in vitro. *Biochem. Biophys. Res. Commun.* **390**, 1334-1339.
Naiche, L. A., Holder, N. and Lewandoski, M. (2011). FGF4 and FGF8 comprise the wavefront activity that controls somitogenesis. *Proc. Natl. Acad. Sci. USA* **108**, 4018-4023.
Narayanan, K., Schumacher, K. M., Tasnim, F., Kandasamy, K., Schumacher, A., Ni, M., Gao, S., Gopalan, B., Zink, D. and Ying, J. Y. (2013). Human embryonic stem cells differentiate into functional renal proximal tubular-like cells. *Kidney Int.* **83**, 593-603.
Ng, E. S., Davis, R., Stanley, E. G. and Elefanty, A. G. (2008). A protocol describing the use of a recombinant protein-based, animal product-free medium (APEL) for human embryonic stem cell differentiation as spin embryoid bodies. *Nat. Protoc.* **3**, 768-776.
Niederreither, K., Subbarayan, V., Dollé, P. and Chambon, P. (1999). Embryonic retinoic acid synthesis is essential for early mouse post-implantation development. *Nat. Genet.* **21**, 444-448.
Nishikawa, M., Yanagawa, N., Kojima, N., Yuri, S., Hauser, P. V., Jo, O. D. and Yanagawa, N. (2012). Stepwise renal lineage differentiation of mouse embryonic stem cells tracing in vivo development. *Biochem. Biophys. Res. Commun.* **417**, 897-902.
Obara-Ishihara, T., Kuhlman, J., Niswander, L. and Herzlinger, D. (1999). The surface ectoderm is essential for nephric duct formation in intermediate mesoderm. *Development* **126**, 1103-1108.
Ortega, S., Ittmann, M., Tsang, S. H., Ehrlich, M. and Basilico, C. (1998). Neuronal defects and delayed wound healing in mice lacking fibroblast growth factor 2. *Proc. Natl. Acad. Sci. USA* **95**, 5672-5677.
Parameswaran, M. and Tam, P. P. L. (1995). Regionalisation of cell fate and morphogenetic movement of the mesoderm during mouse gastrulation. *Dev. Genet.* **17**, 16-28.
Patient, R. K. and McGhee, J. D. (2002). The GATA family (vertebrates and invertebrates). *Curr. Opin. Genet. Dev.* **12**, 416-422.
Patterson, L. T. and Potter, S. S. (2004). Atlas of Hox gene expression in the developing kidney. *Dev. Dyn.* **229**, 771-779.
Preger-Ben Noon, E., Barak, H., Guttmann-Raviv, N. and Reshef, R. (2009). Interplay between activin and Hox genes determines the formation of the kidney morphogenetic field. *Development* **136**, 1995-2004.
Radice, G. L., Rayburn, H., Matsunami, H., Knudsen, K. A., Takeichi, M. and Hynes, R. O. (1997). Developmental defects in mouse embryos lacking N-cadherin. *Dev. Biol.* **181**, 64-78.
Ren, X., Zhang, J., Gong, X., Niu, X., Zhang, X., Chen, P. and Zhang, X. (2010). Differentiation of murine embryonic stem cells toward renal lineages by conditioned medium from ureteric bud cells in vitro. *Acta Biochim. Biophys. Sin.* **42**, 464-471.
Rossant, J., Zirngibl, R., Cado, D., Shago, M. and Giguère, V. (1991). Expression of a retinoic acid response element-hsplacZ transgene defines specific domains of transcriptional activity during mouse embryogenesis. *Genes Dev.* **5**, 1333-1344.
Rumballe, B. A., Georgas, K. M., Combes, A. N., Ju, A. L., Gilbert, T. and Little, M. H. (2011). Nephron formation adopts a novel spatial topology at cessation of nephrogenesis. *Dev. Biol.* **360**, 110-122.
Sainio, K., Hellstedt, P., Kreidberg, J. A., Saxén, L. and Sariola, H. (1997). Differential regulation of two sets of mesonephric tubules by WT-1. *Development* **124**, 1293-1299.
Sajithlal, G., Zou, D., Silvius, D. and Xu, P.-X. (2005). Eya1 acts as a critical regulator for specifying the metanephric mesenchyme. *Dev. Biol.* **284**, 323-336.
Sakai, Y., Meno, C., Fujii, H., Nishino, J., Shiratori, H., Saijoh, Y., Rossant, J. and Hamada, H. (2001). The retinoic acid-inactivating enzyme CYP26 is essential for establishing an uneven distribution of retinoic acid along the anterio-posterior axis within the mouse embryo. *Genes Dev.* **15**, 213-225.
Saxen, L. (1987). *Organogenesis of the Kidney*. Cambridge, UK: Cambridge University Press.
Shamim, H. and Mason, I. (1999). Expression of Fgf4 during early development of the chick embryo. *Mech. Dev.* **85**, 189-192.
Sheng, G. and Stern, C. D. (1999). Gata2 and Gata3: novel markers for early embryonic polarity and for non-neural ectoderm in the chick embryo. *Mech. Dev.* **87**, 213-216.
Short, K. M., Combes, A. N., Lefevre, J., Ju, A. L., Georgas, K. M., Lamberton, T., Cairncross, O., Rumballe, B. A., McMahon, A. P., Hamilton, N. A. et al. (2014). Global quantification of tissue dynamics in the developing mouse kidney. *Dev. Cell* **29**, 188-202.
Song, B., Smink, A. M., Jones, C. V., Callaghan, J. M., Firth, S. D., Bernard, C. A., Laslett, A. L., Kerr, P. G. and Ricardo, S. D. (2012). The directed differentiation of human iPS cells into kidney podocytes. *PLoS ONE* **7**, e46453.
Soshnikova, N. and Duboule, D. (2009). Epigenetic temporal control of mouse Hox genes in vivo. *Science* **324**, 1320-1323.
Steenhard, B. M., Isom, K. S., Cazcarro, P., Dunmore, J. H., Godwin, A. R., St. John, P. L. and Abrahamson, D. R. (2005). Integration of embryonic stem cells in metanephric kidney organ culture. *J. Am. Soc. Nephrol.* **16**, 1623-1631.
Sweetman, D., Wagstaff, L., Cooper, O., Weijer, C. and Münsterberg, A. (2008). The migration of paraxial and lateral plate mesoderm cells emerging from the late primitive streak is controlled by different Wnt signals. *BMC Dev. Biol.* **8**, 63.
Taguchi, A., Kaku, Y., Ohmori, T., Sharmin, S., Ogawa, M., Sasaki, H. and Nishinakamura, R. (2014). Redefining the in vivo origin of metanephric nephron progenitors enables generation of complex kidney structures from pluripotent stem cells. *Cell Stem Cell* **14**, 53-67.
Takada, S., Stark, K. L., Shea, M. J., Vassileva, G., McMahon, J. A. and McMahon, A. P. (1994). Wnt-3a regulates somite and tailbud formation in the mouse embryo. *Genes Dev.* **8**, 174-189.
Takahashi, K., Tanabe, K., Ohnuki, M., Narita, M., Ichisaka, T., Tomoda, K. and Yamanaka, S. (2007). Induction of pluripotent stem cells from adult human fibroblasts by defined factors. *Cell* **131**, 861-872.
Takasato, M., Er, P. X., Becroft, M., Vanslambrouck, J. M., Stanley, E. G., Elefanty, A. G. and Little, M. H. (2014a). Directing human embryonic stem cell differentiation towards a renal lineage generates a self-organizing kidney. *Nat. Cell Biol.* **16**, 118-126.
Takasato, M., Maier, B. and Little, M. H. (2014b). Recreating kidney progenitors from pluripotent cells. *Pediatr. Nephrol.* **29**, 543-552.
Tallquist, M. D., Weismann, K. E., Hellström, M. and Soriano, P. (2000). Early myotome specification regulates PDGFA expression and axial skeleton development. *Development* **127**, 5059-5070.
Thomson, J. A., Itskovitz-Eldor, J., Shapiro, S. S., Waknitz, M. A., Swiergiel, J. J., Marshall, V. S. and Jones, J. M. (1998). Embryonic stem cell lines derived from human blastocysts. *Science* **282**, 1145-1147.
Vetter, S. M. R. and Gibley, C. W. (1966). Morphogenesis and histochemistry of the developing mouse kidney. *J. Morphol.* **120**, 135-155.
Vigneau, C., Polgar, K., Striker, G., Elliott, J., Hyink, D., Weber, O., Fehling, H.-J., Keller, G., Burrow, C. and Wilson, P. (2007). Mouse embryonic stem cell-derived embryoid bodies generate progenitors that integrate long term into renal proximal tubules in vivo. *J. Am. Soc. Nephrol.* **18**, 1709-1720.
Wahl, M. B., Deng, C., Lewandoski, M. and Pourquié, O. (2007). FGF signaling acts upstream of the NOTCH and WNT signaling pathways to control segmentation clock oscillations in mouse somitogenesis. *Development* **134**, 4033-4041.
Wellik, D. M., Hawkes, P. J. and Capecchi, M. R. (2002). Hox11 paralogous genes are essential for metanephric kidney induction. *Genes Dev.* **16**, 1423-1432.
Wijgerde, M., Karp, S., McMahon, J. and McMahon, A. P. (2005). Noggin antagonism of BMP4 signaling controls development of the axial skeleton in the mouse. *Dev. Biol.* **286**, 149-157.
Woolf, A. S. (2009). Embryology. In *Pediatric Nephrology* (ed. E. Avner, W. Harmon, P. Niaudet and N. Yoshikawa), pp. 3-30. Berlin; Heidelberg: Springer.
Xia, Y., Nivet, E., Sancho-Martinez, I., Gallegos, T., Suzuki, K., Okamura, D., Wu, M.-Z., Dubova, I., Esteban, C. R., Montserrat, N. et al. (2013). Directed differentiation of human pluripotent cells to ureteric bud kidney progenitor-like cells. *Nat. Cell Biol.* **15**, 1507-1515.
Xu, J., Wong, E. Y. M., Cheng, C., Li, J., Sharkar, M. T. K., Xu, C. Y., Chen, B., Sun, J., Jing, D. and Xu, P.-X. (2014). Eya1 interacts with Six2 and Myc to regulate expansion of the nephron progenitor pool during nephrogenesis. *Dev. Cell* **31**, 434-447.
Yamaguchi, T. P., Bradley, A., McMahon, A. P. and Jones, S. (1999). A Wnt5a pathway underlies outgrowth of multiple structures in the vertebrate embryo. *Development* **126**, 1211-1223.

Yamamoto, M., Cui, L., Johkura, K., Asanuma, K., Okouchi, Y., Ogiwara, N. and Sasaki, K. (2006). Branching ducts similar to mesonephric ducts or ureteric buds in teratomas originating from mouse embryonic stem cells. *Am. J. Physiol. Renal Physiol.* **290**, F52-F60.

Yang, X., Dormann, D., Münsterberg, A. E. and Weijer, C. J. (2002). Cell movement patterns during gastrulation in the chick are controlled by positive and negative chemotaxis mediated by FGF4 and FGF8. *Dev. Cell* **3**, 425-437.

Yang, X., Chrisman, H. and Weijer, C. J. (2008). PDGF signalling controls the migration of mesoderm cells during chick gastrulation by regulating N-cadherin expression. *Development* **135**, 3521-3530.

Yatskievych, T. A., Ladd, A. N. and Antin, P. B. (1997). Induction of cardiac myogenesis in avian pregastrula epiblast: the role of the hypoblast and activin. *Development* **124**, 2561-2570.

Yoshikawa, Y., Fujimori, T., McMahon, A. P. and Takada, S. (1997). Evidence that absence of Wnt-3a signaling promotes neuralization instead of paraxial mesoderm development in the mouse. *Dev. Biol.* **183**, 234-242.

Yun, K., Ajima, R., Sharma, N., Costantini, F., Mackem, S., Lewandoski, M., Yamaguchi, T. P. and Perantoni, A. O. (2014). Non-canonical Wnt5a/Ror2 signaling regulates kidney morphogenesis by controlling intermediate mesoderm extension. *Hum. Mol. Genet.* **23**, 6807-6814.